Bad Aibling , June 13, 2000

Steffen Hein

Spinner GmbH. München
Aiblinger Str. 30, DE-83620 Feldkirchen-Westerham, Germany

Gauge techniques in time and frequency domain TLM

Abstract. Typical features of the Transmission Line Matrix (TLM) algorithm in connection with stub loading techniques and prone to be hidden by common frequency domain formulations are elucidated within the propagator approach. In particular, the latter reflects properly the perturbative character of the TLM scheme and its relation to gauge field models. Internal 'gauge' degrees of freedom are made explicit in the frequency domain by introducing the complex nodal S-matrix as a function of operators that act on external or internal fields or virtually couple the two. As a main benefit, many techniques and results gained in the time domain thus generalize straight away. The recently developed deflection method for algorithm synthesis, which is extended in this paper, or the non-orthogonal node approximating Maxwell's equations, for instance, become so at once available in the frequency domain. In view of applications in computational plasma physics, the TLM model of a relativistic charged particle current coupled to the Maxwell field is traced out as a prototype. **MSC-classes**: 65C20, 65M06, 76D05

Keywords: Gauge techniques, perturbative schemes, TLM method, propagator approach, plasma physics

1. Introduction

When P. B. Johns and coworkers introduced the transmission line matrix (TLM) numerical method in the early seventies [7] they were certainly not aware of handling gauge field concepts. In fact, the perturbative aggregation of internal gauge degrees of freedom plays a salient role in TLM in the form of 'stub loading'. This well known technique, ad hoc applied in a great many variants to model continuous mesh deformations or material parameters, e.g., expands to a powerful framework that allows for a systematic integration of manifold interactions. Stubs in a generalized sense may for instance add mass to a field much alike a Higgs field [15], or induce superconducting or non-reciprocal behaviour [13],[14]. Very much of the strength and versatility of TLM rests on this feature that indeed relates the method to some pioneering developments in modern particle physics.

Varied formal characterizations of the TLM scheme have been given since the early transmission line network interpretations. Some authors proceed from Huygens' principle [8] (sometimes misunderstood) others use concepts of state space control theory [10] or random walk [2], [9]. The present paper is not intended to add a further characterization to these and alternate

interpretations which are usually built on the cinematics of a special kind of propagating quantities (waves, particles, temperatures etc.). Instead, this study focusses on the internal structure of the TLM algorithm irrespective of its physical interpretation. It nevertheless remains remarkable that so many heterogeneous perceptions exist and apparently match the algorithmic scheme of the method. The perturbative structure of TLM, with its gauge fixture not at least, certainly explains much of that multiplicity.

With sustained evolution of computer performance in coming years there will be an increasing need of highly flexible numerical schemes, complementary to powerful standard solvers. The versatile structure and the diversity of yet known applications in wave propagation [1], chemical reaction-diffusion [10], heat transfer [9], plasma physics [15], and further domains provide some evidence that the TLM method can play a competent role on the court.

This requires, however, a refined technical outfit being built on sound mathematics. Theorems like the deflection lemma [14], a generalized version of which is given in this paper, should constitute a canonical basis for algorithm synthesis. The usage and usefulness of those tools amenable to the propagator approach [11] have already been shown up within a series of numerical applications [12] - [15]. On the issue of this paper the TLM model of a relativistic charged particle current coupled to the Maxwell field provides supplementary illustration.

2. The algorithm and its interpretation

This section is widely heuristic and starts slightly outside our subject. Conceptually, the TLM algorithm will be separated from its interpretation in terms of any modelled fields. This obviously implies outlining a canonical passage between two severed parts: physical fields and computed quantities. The TLM typical manner of generating these quantities, i.e. the computational part, is then headed for necessarily on a level of abstraction beyond the commonly considered Maxwell field.

It is in the obvious nature of any splittings (conceptual just as physical) that junctions appear double faced, and so the joints between the TLM algorithm and its interpretation, viz. ports and nodes in cells, take a twofold role. So it has to be clarified what is meant in either context.

At the interface to physical fields in space a *cell* stands for a convex polyhedron in configuration space $\mathbb{R}^D$ and a *port* for a distribution, i.e. a continuous linear functional acting on a field, with its support on a closed subset of the cell boundary (a point, line segment, or face e.g.). The distributional support is also referred to as the *location* of that port. If no confusion can arise it will be simply identified with the port.

Again, in the same context, the *node* comprises the family of all port distributions of a cell, yet shifted by translations into its interior (where conceptually one effective internal state of the cell at a time interacts with boundary states - this touches the algorithmic role of ports and nodes treated

below). Note that in many cases distributed integrals instead of point supported functionals, viz. the shifted *nodal images* of the ports, probe the fields in the cells.

In a condensed slightly formalized writing: Every port p of a cell together with the node gives rise to a pair of linear forms (p, Z), $(p, Z)^{\sim}$ which probe a real or complex vector field $Z = (Z_1, \ldots, Z_m)$; $m \in \mathbb{N}_+$, at the cell boundary and within the cell. The two forms are naturally interrelated by pull-back

$$(1) \qquad (\, p, Z\,)^{\sim} \quad = \quad (\, p \circ s, Z\,) \quad = \quad \left(\, p, Z \circ s^{-1}\right)$$

where s denotes the pertinent translational shift of the port onto its nodal image, cf. fig 1. Defining these forms consistently as distributed or point supported functionals (*finite integrals*, e.g.) is a constituent part of any interpretation of the TLM model.

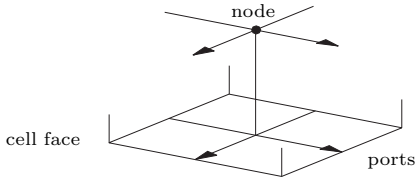

Figure 1: Cell boundary ports and their nodal images

Quite different, and still more abstract, are the roles of ports, nodes, and cells in the computational context. Every cell stands here for a direct sum (viz. a triple) of linear spaces, which respectively represent observable *link* states in the cell or on its boundary, and unobservable *gauge* (or *stub*) degrees of freedom. Observable vectors $z_\mu^{p,n}$ are labelled by ports p or their nodal images n, and are linearly interrelated to physical fields by an interpretation. In a more precise diction, an *interpretation* may be defined as a family of linear maps I_ζ, indexed by the cells of a *mesh*, with domain a distinguished class of vector fields in configuration space which represent physical fields and with their range in the set of observable cell states:

$$(2) \qquad I_\zeta : Z_\mu \to \left(z_\mu^{p,n}\right) \;;\; z_\mu^p = (\, p_\mu, Z_\mu)\,, \quad z_\mu^n = (\, p_\mu, Z_\mu)^{\sim}$$

(μ labels the ports and pertinent fields in cell ζ and superscripts p, n refer respectively to ports on the cell boundary or to their nodal images in the cell - a port being counted here as many times as it acts on a different field.) Note that no fixed linear relations of such a kind interconnect any gauge vectors with fields.

Ultimately, and by it most markedly characterizing the TLM scheme, the ports together with their nodal images represent scattering channels for states incident at the cell boundary and scattered in the node. As a scattering channel every common port of two adjacent cells thus naturally connects their nodes, i.e. constitutes a *link*.

The inherent scattering scheme of the algorithm postulates in the line of Lax-Phillips [3] a direct splitting of the link states into incoming and

outgoing components

$$z = z_{in} \oplus z_{out} \tag{3}$$

which of course has to be defined in harmony with the propagation properties of the modelled fields. In reference [14] the details are carried through for the Maxwell field, for example. The Poynting vector evaluated at the cell faces yields there a canonical splitting and a quadratic form that is positive or negative, respectively, on the incoming or outgoing subspaces.

In TLM diction the latter are usually called the (spaces of) incident and reflected quantities and in the following π_{in}, π_{out} denote the pertinent projections.

The TLM scattering algorithm, which is eo ipso perturbative, solves finite difference equations in the form of model equations between states that in any interpretation should approximate physical fields (i.e. solutions of integro-differential equations) in any sense and order (sect.4). This is the requirement of *consistence*, as a cardinal property of the interpretation.

In contrast, the question of internal convergence, which is essentially that of computational *stability*, refers to intrinsic properties of the TLM algorithm such as are subject of this paper. That question has thus to be taken up in due course. (We are not unhappy that it is in general easier.)

3. The propagator relations

Causality requires in the time domain the scattered states of a cell to be functions of previously incident states. With a cell dependent *reflection operator* $\mathcal{R}$ the outgoing port quantities are thus

$$z^p_{out}(t+\tau) = \mathcal{R}\left(z^p_{in}(t-\mu\tau)\right)_{\mu\in\mathbb{N}} \tag{4}$$

where τ denotes the time step. (Suitable definitions release from introducing line impedances, such as are commonly used instead of the projections (3) - in fact they are substitutes for projections, cf. the appendix.) $\mathcal{R}$ assembles the physical interactions within the cell in a geometry dependent manner, and represents in this sense the TLM system *locally*, while the *global* topological structure, as given by the port linking scheme and the boundary conditions, are brought in by the *connection map* $\mathcal{C}$. At every time step the latter transmits the reflected port quantities to adjacent cells or, at a system boundary, back into the same cell and contingently adds the field excitations by acting linearly as

$$\left(z^p_{in}\right)_\zeta = \mathcal{C}\left(\left(z^p_{out}\right)_\eta, \left(z^p_{exc}\right)_\vartheta\right) \tag{5}$$

where ζ, η, ϑ label the cells and z^p_{exc} denotes any excitation.

Short-cut, every pair $(\mathcal{C}, \mathcal{R}_\zeta)$ consisting of a connection map $\mathcal{C}$ and a family $\mathcal{R}_\zeta$ of reflection operators labelled by the cells of the same mesh will be referred to as a *TLM system*.

The interesting objects in a TLM system are, of course, the causal operators $\mathcal{R}_\zeta$ which like the pages of a book are merely bound together by the 'book binding' function $\mathcal{C}$. In addition to being defined on back-in-time running sequences of incident states, $\mathcal{R}$ may itself depend on time and may be non-linear. Before venturing on the TLM typical structure of $\mathcal{R}$ a glance is cast at some cinematical relations between port and node quantities.

Operationally, the TLM approach, as a genuine scattering scheme, splits off a cinematical part from the dynamical evolution by handling some interactions as a perturbation. In classical Lax-Phillips scattering, for instance, two 'intertwingled' one parameter unitary groups describe respectively the free and interacting dynamics [3]. A related ansatz leads in perturbative quantum field theory to the Dyson expansion of S-parameters in the form of Feynman diagrams which again couple free fields [4]. Technically, the TLM algorithm operates similarly with freely propagating port and node quantities that before and past reflection are forced into fixed phase relations by imposing in the time domain

$$z^n_{in}\,(t) := z^p_{in}\,(\,t - \frac{\tau}{2}\,) \quad , \quad z^n_{out}\,(t) := z^p_{out}\,(\,t + \frac{\tau}{2}\,) \tag{6}$$

Note well that these are technical arrangements to enable the scattering scheme, while only total quantities,

$$z^{p,n} = z^{p,n}_{in} \oplus z^{p,n}_{out} \quad , \qquad cf. \quad (3) \tag{7}$$

represent observable states and in fact enter the model equations (cf. sect.4).

Scarce and innocent as they appear, settings (4, 5, 6) together with (3) contain yet very much of the substance of TLM. On the basis of essentially these ingredients, which form the core issues of the so-called propagator approach [11], [15], internal 'gauge' degrees of freedom arise naturally on introducing additional interactions by a perturbation, along with S-parameters that couple these to the original states. A simple way of giving a rigorous meaning to that is the deflection lemma. Originally introduced in reference [14], the lemma is subsequently generalized to handle higher order equations.

4. The deflection lemma

Finite difference equations that in the form of *model equations* approximate the dynamical equations of any physical interpretation interrelate in the time domain sequences of total node and port quantities

$$[z^{n,p}] = (z^{n,p}\,(t - \mu\tau))_{\mu=0,1,2,\ldots} \tag{8}$$

which represent observable states in the cell and on its boundary, at present time t and in their history. A maximum μ that eventually enters the equations obviously reflects the temporal order of the modelled dynamical problem, which may be finite or infinite. To *any* order the model equations can be written

$$\mathcal{F}[z^n_+][z^p] = 0 \tag{9}$$

with a suitable causal operator $\mathcal{F}$ (where *causal* stands always for being defined on back-in-time running sequences such as (8)). subscript $+(-)$ denotes a $\tau/2$ time shift

$$[z^{n,p}_{+(-)}] := [z^{n,p}]_{t+(-)\frac{\tau}{2}} = \left(z^{n,p}\left(t+(-)\frac{\tau}{2}-\mu\tau\right)\right)_{\mu\in\mathbb{N}} \tag{10}$$

which in harmony with the phase relations (6) synchronizes port and node switching in equations (9), for every vector $z^p_{in}(t)$ incident at a cell and constant on each time interval $[k\tau,(k+1)\tau)$; $k\in\mathbb{Z}$. Note that $\mathcal{F}$ may itself be time dependent in like manner, i.e. as a time step function matching integer multiples of τ.

In the literature equations (9) are encountered in manyfold guises. For instance, in reference [11] Maxwell's integral equations discretized in a convex hexahedral cell of else arbitrary shape take the form

$$\psi_0 z^p(t) = \varphi_0 z^n\left(t+\frac{\tau}{2}\right) + \varphi_1 z^n\left(t-\frac{\tau}{2}\right) \tag{11}$$

where $z=(\mathbf{u},\mathbf{i})$ represent finite integrals over electric and magnetic field strengths, ψ_0 essentially interchanges $\mathbf{u}$ and $\mathbf{i}$ and φ_0, ψ_0 are selfadjoint $\mathbb{R}$-linear operators, cf. references [14],[15] and the appendix of this paper.

By saying that a TLM system $(\mathcal{C},\mathcal{R}_\zeta)$ generates solutions of equations (9) it is meant that the total fields $z^{n,p}$, cf.(3,7), satisfy the equations for *all* vectors z^p_{in} incident at any cell (and as step functions of time of course matching τ). Obviously, this defines a *local*, so far purely algebraic property of the TLM system, i.e. one referring to $\mathcal{R}_\zeta$ and indepedent of $\mathcal{C}$ that still disregards all questions of convergence or computational stability, for instance. As a rule, the TLM system solving (9) depends strongly on the time step and additional contraction properties must be checked on selecting a particular stable system (cf. sect.5).

The deflection lemma establishes general recurrence relations between solutions of model equations that differ by a perturbation.

Let a TLM system $(\mathcal{C},\mathcal{R}_\zeta)$ generate solutions of equation (9) with any $\mathcal{F}$ of the form

$$\mathcal{F}[z^n_+][z^p] = \sum_{\mu\in\mathbb{N}} \varphi_\mu z^n\left(t+\frac{\tau}{2}-\mu\tau\right) + \psi_\mu z^p(t-\mu\tau) \tag{12}$$

wherein φ_μ, ψ_μ are $\mathbb{R}$-linear operators (many if not almost all of which may be zero). Consider then a perturbation of equation (9) by a causal possibly non-linear operator $\mathcal{J}$ that maps into the image space of $\mathcal{F}$ (i.e. φ_μ, ψ_μ and $\mathcal{J}$ share the same image space). $\mathcal{F}$ and $\mathcal{J}$ may be time dependent, i.e. step functions of time matching τ.

Then one can state the following

Proposition (Deflection Lemma) A TLM system $(\mathcal{C},\mathcal{R}^\sim_\zeta)$, with the same connection map as above, generates solutions of equation

$$\mathcal{F}[z^n_+][z^p] = \mathcal{J}[z^n_-][z^p] \tag{13}$$

if and only if the *deflection*

$$\mathcal{D} := \mathcal{R}^{\sim} - \mathcal{R} \tag{14}$$

satisfies recursively

$$\varphi_{o,t}\mathcal{D}_t = -\mathcal{J}_t[z^n_-]\,[z^p] - \sum_{\mu\in\mathbb{N}_+} \left(\varphi_\mu + \psi_{\mu-1}\right)_t \mathcal{D}_{t-\mu\tau} \tag{15}$$

Corollary. Let φ_0 be injective (one to one) on the outgoing subspace and assume $\varphi_0 \circ \pi_{out}$ covers the ranges of $\mathcal{J}$, $\varphi_\mu \circ \pi_{out}$, and $\psi_\mu \circ \pi_{out}$; $\mu \in \mathbb{N}$. Then

$$\mathcal{D}_t := -\left(\varphi_0 \circ \pi_{out}\right)^{-1}_t \ \{\ \mathcal{J}_t[z^n_-][z^p] + \sum_{\mu\in\mathbb{N}_+} \left(\varphi_\mu + \psi_{\mu-1}\right)_t \mathcal{D}_{t-\mu\tau}\ \} \tag{16}$$

defines recursively a causal operator $\mathcal{D}$ such that

$$\mathcal{R}^{\sim} := \mathcal{R} + \mathcal{D}$$

is the reflection map of a TLM system $(\mathcal{C},\, \mathcal{R}^{\sim}_{\zeta})$ which generates solutions of equation (13).

Moreover, if $\mathcal{D}_0 \equiv 0$, then this system is the *unique* one which branches from $(\mathcal{C}, \mathcal{R}_\zeta)$ at $t = 0$, i.e. that initially coincedes with the unperturbed system.

Condensed statements of that kind support a comment before being proved:

Guided by conceivable applications the perturbation $\mathcal{J}$ is written as a function of total port and node states and of time. Most commenly, it is a function of nodal states only.

If $\varphi_0 \circ \pi_{out}$ is invertible, then the negative time shift in (13) makes $\mathcal{J}_t$ depend on nodal states up to

$$z^n\left(\, t - \frac{\tau}{2}\,\right) = z^p_{in}\left(t-\tau\right) + \mathcal{R}^{\sim}\left[z^p_{in}\right]_{t-\tau} = z^p_{in}\left(t-\tau\right) + \mathcal{R}\left[z^p_{in}\right]_{t-\tau} + \mathcal{D}_{t-\tau} \tag{17}$$

thus ensuring that $\mathcal{D}$ enters the right-hand side of recursion (16) (implicitely in the argument of $\mathcal{J}_t$) up to $\mathcal{D}_{t-\tau}$ at most, rather than up to $\mathcal{D}_t$ which obviously would lead to ill-defined recurrence relations without further severe restrictions on $\mathcal{J}$.

Note that from $\mathbb{R}$-linearity only additivity of φ_μ, ψ_μ enters the following

Proof Let hence $(\mathcal{C}, \mathcal{R}_\zeta)$ generate solutions of (9) and let for a second TLM system $(\mathcal{C}, \mathcal{R}^{\sim}_{\zeta})$ the deflection $\mathcal{D}$ be defined by (14). Then for every sequence of states $[z^p_{in}]$ incident at a cell the total states of the second system are

$$\begin{aligned} \tilde{z}^p\left(t\right) &= z^p_{in} + \mathcal{R}^{\sim}\left[z^p_{in}\right]_{t-\tau} \\ &= z^p_{in} + \mathcal{R}\left[z^p_{in}\right]_{t-\tau} + \mathcal{D}_{t-\tau} \\ \tilde{z}^n\left(t + \tfrac{\tau}{2}\right) &= z^p_{in} + \mathcal{R}\left[z^p_{in}\right]_t + \mathcal{D}_t \end{aligned} \tag{18}$$

This substituted for $z^{n,p}$ in equation (13) yields

$$\begin{aligned}\mathcal{F}[\tilde{z}^p_+][\tilde{z}^p] &= \textstyle\sum_{\mu\in\mathbb{N}} \{\ \varphi_\mu(z^p_{in}(t-\mu\tau) + \mathcal{R}[z^p_{in}]_{t-\mu\tau} + \mathcal{D}_{t-\mu\tau}) \\ &\quad +\psi_\mu(z^p_{in}(t-\mu\tau) + \mathcal{R}[z^p_{in}]_{t-\tau-\mu\tau} + \mathcal{D}_{t-\tau-\mu\tau})\} \\ &= \textstyle\sum_{\mu\in\mathbb{N}} \{\ \varphi_\mu(z^n(t+\frac{\tau}{2}-\mu\tau) + \mathcal{D}_{t-\mu\tau}) \\ &\quad +\psi_\mu(z^p(t-\mu\tau) + \mathcal{D}_{t-\tau-\mu\tau})\} \\ &= \mathcal{J}_t[\tilde{z}^n_-][\tilde{z}^p]\end{aligned} \tag{19}$$

By virtue of the additivity of φ_μ, χ_μ follows

$$\mathcal{F}[\tilde{z}^n_+][\tilde{z}^p] = \mathcal{F}[z^n_+][z^p] + \sum_{\mu\in\mathbb{N}} \varphi_\mu \mathcal{D}_{t-\mu\tau} + \psi_\mu \mathcal{D}_{t-\tau-\mu\tau} = \mathcal{J}_t[\tilde{z}^n_-][\tilde{z}^p] \tag{20}$$

Equation (9) states that $\mathcal{F}[z^n_+][z^p]$ above vanishes and inspection of the remaining terms yields the proposition.

5. The S-matrix propagator

The first order linear equation (11) admits a solution in closed form as an iterated scattering process. This has been pointed out in detail in references [14], [15] at the example of the non-orthogonal Maxwell field model. Using the commuting family of projections which split the state space of each cell ζ, with identity operator Id_ζ, into observable link states and unobservable gauge or stub vectors

$$Id_\zeta = \pi_l \oplus \pi_s \tag{21}$$

and then again the link states into incoming and outgoing subspaces of port and node quantities

$$\pi_l = \pi_{in} \oplus \pi_{out} \tag{22}$$

the reflection map of the first order linear process solving (11) is

$$\begin{aligned} z^p_{out}(t+\tau) = \mathcal{R}\,[z^p_{in}] \ &= \ z^n_{out}\ (\ t + \frac{\tau}{2}\ ) \\ &= \pi_{out}\ S\ z^n_{in}\ (\ t+\frac{\tau}{2}\ ) \\ &\quad + \pi_{out}\ S\ \sum_{\mu=1}^{\infty} (\pi_s S\ )^\mu\ z^n_{in}\ (\ t+\frac{\tau}{2}-\mu\tau\ ) \end{aligned} \tag{23}$$

S denotes the nodal scattering operator which acts between in and outgoing node and stub vectors and can thus be written

$$S = (\pi_{out} \oplus \pi_s)\, S\, (\pi_{in} \oplus \pi_s) = K + L + M + N \tag{24}$$

where as usual

$$K := \pi_{out} S \pi_{in}, \quad L := \pi_{out} S \pi_s, \quad M := \pi_s S \pi_{in}, \quad N := \pi_s S \pi_s \tag{25}$$

have been introduced. With these operators equation (23) reads more concisely

$$z^n_{out}(t) = K z^n_{in}(t) + L \sum_{\mu=0}^{\infty} N^\mu M z^n_{in}(t - (\mu+1)\tau) \tag{26}$$

(graphically represented in fig.2a).

K, L, M, N are easily determined from equation (11) by substituting for $z^{n,p} = z^{n,p}_{in} + z^{n,p}_{out}$ in this equation the total scattering response of a Dirac pulse

$$z^p_{in}(t) = z^n_{in}(\, t + \frac{\tau}{2}\,) = \begin{cases} z_0 \;\; if & t \in [o, \tau) \\ 0 \;\; else & \end{cases} \tag{27}$$

applied and added to (23, 26). By evaluating equations (11) with these replacements at time intervals $[k\tau, (k+1)\tau)$, $k \in \mathbb{N}$, provides operator identities that are independent for $k = 0, 1$ and $k \geq 2$ under rather general conditions, cf. [12] - [15] and which allow to determine K uniquely, while L,M, and N are unique at most up to a linear automorphism of the stub space. Indeed, sheer inspection of the scattering response (23, 26) makes clear that any invertible linear transformation G of the stub space yields an equivalent scattering representation of $\mathcal{R}$ if S is replaced by

$$S' := K + L' + M' + N' \tag{28}$$

with $L' := LG^{-1}$, $M' := GM$, $N' := GNG^{-1}$. It is this property that led to the understanding of stub vectors as internal *gauge* degrees of freedom, the automorphisms of the stub linear space (in transmission line parlance: a group of generalized impedance transformations) constituting the pertinent *gauge group*.

As already mentioned, the inherent gauge features of the TLM scheme can actually be traced back to the deflection lemma, the latter displaying in like manner the generation mechanism for stub degrees of freedom as rather suggestively also their gauge property.

Given a TLM system $(\mathcal{C}, \mathcal{R}_\zeta)$ that generates solutions of equations (9) with any operator φ_0 sharing the technical prerequisites refered to, it is a straightforward exercise applying the lemma and its corollary to write down the updating instructions for a 'deflected' system $(\mathcal{C}, \mathcal{R}^\sim)$ that solves the perturbed equations (13):

$$\begin{aligned} z^p_{out}(t+\tau) &:= \mathcal{R}_t[z^p_{in}] + \mathcal{D}(t) \\ I(t+\tau) &:= -(\varphi_0 \circ \pi_{out})^{-1}_{t+\tau} \, \partial_{t+\tau}[z^n_+][z^p] \\ \mathcal{D}(t+\tau) &:= I(t+\tau) - (\varphi_0 \circ \pi_{out})^{-1}_{t+\tau} \sum_{\mu \in \mathbb{N}} (\psi_\mu + \varphi_{\mu+1})_{t+\tau} \, \mathcal{D}(t - \mu\tau) \end{aligned} \tag{29}$$

with all updating operations done in this order and implicitly after the first line

$$z^n\left(t+\tfrac{\tau}{2}\right) = z^p_{in}\left(t\right) + z^p_{out}\left(t+\tau\right)$$

Besides the proper interaction term I, which essentially appears in the model equations (13) and is thus amenable to a direct physical interpretation, the deflecting field $\mathcal{D}$ introduces additional degrees of freedom that in general remain without counterparts in the equations.

The gauge character of the deflection field is suggestively illustrated within scattering representations (23,26) for $\mathcal{R}$ and $\mathcal{R}^\sim$ - assuming for once that such exist. If $S^\sim$ denotes the S-matrix of $\mathcal{R}^\sim$, then it admits a block decomposition in matrix form

$$S^\sim = \left(\begin{array}{c|c} S & L^\sim \\ \hline M^\sim & N^\sim \end{array}\right) \tag{30}$$

wherein S represents the S-matrix of $\mathcal{R}$ and $L^\sim$, $N^\sim$ act on the additional deflection field $\mathcal{D}$. The updating instructions (29) obviously fit with $L^\sim$ of the form

$$L^\sim = \begin{pmatrix} 1 & & & \\ & \ddots & & \\ & & 1 & 0\ldots 0 \end{pmatrix}^T \tag{31}$$

(all other matrix elements of $L^\sim$ being zero). Any invertible transformation G, according to (28) simultaneously applied to $L^\sim$, $M^\sim$ and $N^\sim$, then cannot alter $\mathcal{R}^\sim$ and thus yields an equivalent representation. (The reader may trace this forth to a set of modified updating equations (29).)

Spatial deformations of the TLM mesh continously get through stubs. In fact they are modelled using stubs [1], [8], [12]. Therefore smooth connections between mesh point dislocations and infinitesimal impedance transformations G exist that textually complete the gauge field analogy in the sense of fibrations [5].

Once the gauge fixture of TLM being made available, full advantage can be taken of its power and flexibility. Aside from the nonlinear potentiality opened by the deflection lemma, manifold variants of the linear scheme (26) are conceivable. For instance the generalized ansatz

$$z^n_{out}(t) = K z^n_{in}(t) + \sum_{\kappa=1}^{k} L_\kappa \sum_{\mu\in\mathbb{N}} N^\mu_\kappa M_\kappa z^n_{in}\left(t-(\mu+\kappa)\,\tau\right) \tag{32}$$

(which is graphically depicted in fig.2b) is suited to solve linear model equations of the class (12) with time differences in the port states up to order k.

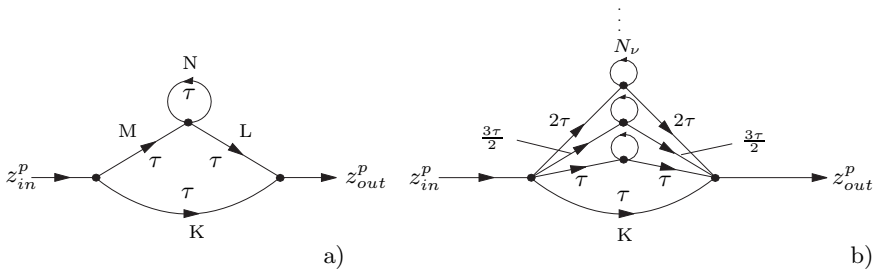

Figure 2: Linear scattering schemes
Every path from left to right following the arrows yields a delayed or phase shifted contribution to the scattering response. (Loops may be repeatedly run through any number of times.)

A direct way to prove the above statement and to derive S-matrix blocks K, L_κ, M_κ and N_κ in (32) is again by evaluating equation (12) at successive time steps for an incident Dirac pulse (27).

6. The stable process in the time and frequency domain

Parallel to the TLM typical splitting of states into link and gauge degrees of freedom external and internal conditions for computational stability may be distinguished, which respectively stress some physical aspects and a purely numerical origin of instability.

In any interpretation the total link vectors are directly related to physical quantities that are in general subjugate to conservations laws. It is hence merely a strengthened consistence postulate to require that the reflection map of each cell must comply with these laws. The entire reflection response of an incident Dirac pulse integrated over time has for instance to be physically balanced with the input.

Actually this goes along with the Lax-Phillips contraction conditions [3] which are sufficient to prevent the observable fields from increasing indefinitely in the mesh. To implement these conditions numerically in the TLM specifical fashion, internal algorithm stability has in addition to prevent gauge fields (i.e. the 'stub quantities') from piling up to infinity. For instance, in a stable non-linear perturbed process which solves equation (13) the deflection must die out in time for any transitory incident fields that do not pass over a certain level.

A universal condition that guarantees computational stability, even in the non-linear case (at least up to some maximum level of incidence), is quite evidently all updating operations must be contractive in a neighbourhood of zero. For the linear processes (26), (32) the operators $N_{(\kappa)}$ control updating between gauge fields. Hence a sufficient condition for internal stability of these processes is

$$\| N \| < 1 \tag{33}$$

if the norm $\| \ldots \|$ is submutiplicative, i.e. characterized by

$$\| N^\mu \| \leq \| N \|^\mu , \qquad \mu \in \mathbb{N} \tag{34}$$

The sup-norm with respect to any state space norm $\| z \|$

$$\| N \|_{\sup} := \sup_{\|z\|=1} \| Nz \| \tag{35}$$

or the Hilbert (spectral) norm

$$\| N \|_H := \max_{\lambda \, eigenvalue \, of \, N} | \lambda |$$

are, for instance, submultiplicative in the sense of (34). All operator norms occurring in the following are tacitely assumed to share this property.

Condition (33) is in general realized in the cases of interest by introducing bounds for the time step. In the frequency domain, for a process of angular frequency $\omega = 2\pi f$, i.e.

$$z^p_{in,out}(t + \mu\tau) = e^{j\omega\mu\tau} z^p_{in,out}(t) , \qquad \mu \in \mathbb{Z} \tag{36}$$

equation (26) reads

$$z^n_{out} = \left(K + L \sum_{\mu=0}^{\infty} N^\mu M e^{j\omega(\mu+1)\tau} \right) z^n_{in} \tag{37}$$

With $\mathbb{C}$-linear operators K, L, M, N this turns into

$$z^n_{out} = \left(K + e^{-j\omega\tau} L \sum_{\mu=0}^{\infty} \left(e^{-j\omega\tau} N \right)^\mu M \right) z^n_{in} \tag{38}$$

A stable process, characterized by condition (33), ensures that the power series in $e^{-j\omega\tau}N$ converges to $(Id - e^{-j\omega\tau}N)^{-1}$. Equations (38) thus becomes $z^n_{out} = S^{\sim} z^n_{in}$ with

$$S^{\sim} = K + L \left(e^{j\omega\tau} Id - N \right)^{-1} M \tag{39}$$

Evidently, in the frequency domain the complex S-matrix connects directly incident with outgoing fields and stubs do no longer enter the algorithm in the form of explicitely computed quantities. Instead, the stubs yield implicitely an additive contribution to the S-matrix

$$S^{\sim}_g = L \left(e^{j\omega\tau} Id - N \right)^{-1} M \tag{40}$$

extracted from decomposition (39). It is virtually this gauge contribution that anew characterizes the TLM scheme here in the frequency domain.

Of course, knowing the nodal S-parameters of each cell, 'intrinsic S-matrices' of entire mesh systems can be computed, just as then S-parameters for any combination of submeshes. (Proceeding in that direction opens

rather a special field of application to linear network theory than deeper structural insight into the TLM method).

In the frequency domain the TLM algorithm solves the eigenvector equation

$$\left(\mathcal{C}S_\zeta^{\sim} e^{j\omega\tau} - Id\right)(z_{in})_\zeta = 0 \tag{41}$$

where ζ runs over all mesh cells and the connection map $\mathcal{C}$ interlaces a steady state excitation which may be imposed on the mesh boundary according to any mode templates for instance.

Various methods for solving equations (41) are imaginable. We experimented with classical conjugate gradient schemes, such as Fletcher-Reeves and Polak-Ribière which, however, showed poor convergence for larger mesh systems of several thousand cells. Very satisfactory results have been obtained, in contrast, with a fixed point iteration analogous to a static time domain process (of course with complex fields). Indeed, reiterating the instructions

$$\begin{aligned}(z_{in})_{\zeta,k} &= \mathcal{C}\,(z_{out} + z_{exc})_{\zeta,k}\\ (z_{out})_{\zeta,k+1} &= e^{j\omega\tau} S_\zeta^{\sim}\,(z_{in})_{\zeta,k}\end{aligned} \tag{42}$$

converges for any steady state excitation $(z_{exc})_\zeta$ quite rapidly to a fixed point, and thus to a solution of equation (41) which matches the imposed excitation pattern. Still faster convergence had been attained by starting with zero fields and smoothly approaching the steady state excitation over a transitory phase of some hundred iterations.

Fig.3 displays convergence thus attained for a 3 dB waveguide directional Riblet coupler.

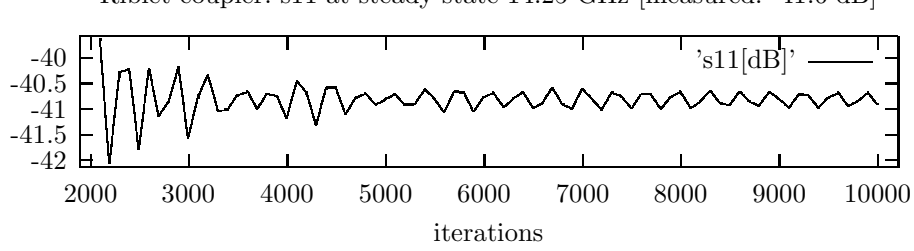

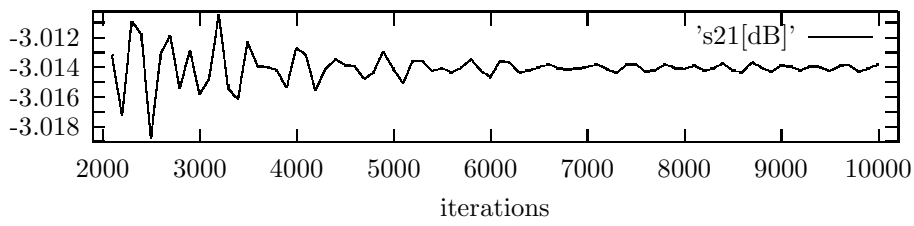

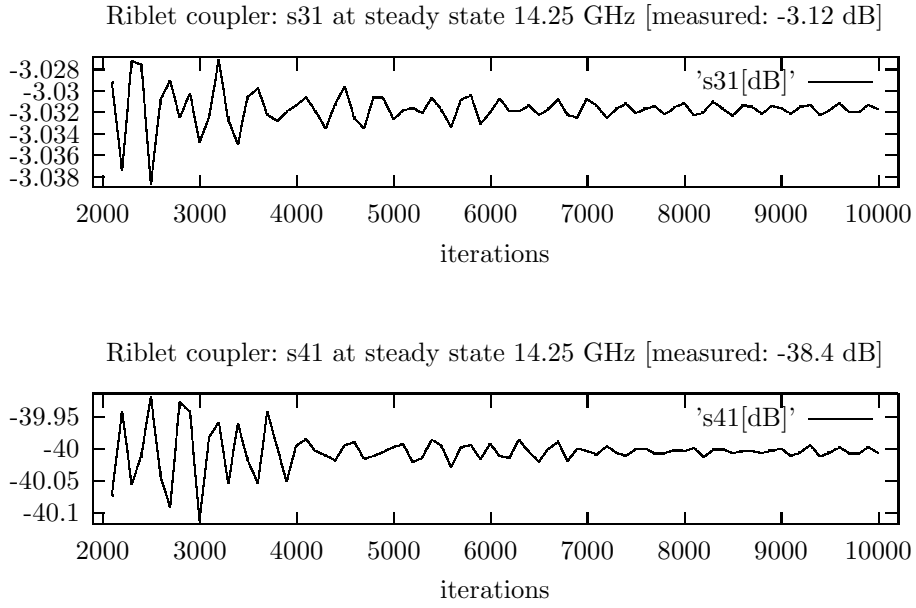

Figure 3: Convergence in the frequency domain of a fixed point iteration (42) for a 3dB waveguide directional coupler (Riblet coupler). The deviations from measurements at the real coupler are mainly due losses, which are neglected in the computational model.

7. Charged particles coupled to the Maxwell field

It has been stressed that this study focusses on the intrinsic structure of the TLM algorithm, not on any interpretation. Still one application is sketched in this section to illustrate the excellent capacity of TLM to cooperate with a tied finite difference scheme. Beyond that, a variety of original research applies concepts of this paper and should be consulted for technical illustration. In particular, part of references [11] - [15] constitute by now 'standard technicality' which can be referred to in the following. (A bridge between the non-orthogonal Maxwell field model, as treated in [15], and the presently generalized formalism is built in the appendix.)

The following application extends the Maxwell field model in a non-linear fashion. By deflection, a relativistic charged particle current is coupled to the apriori free electromagnetic field. The underlying dynamical relations are thus Maxwell's equations and the equations of motion for a particle current with interactions being brought in by Ampère's law and the Lorentz force.

The relativistic mass of a particle at velocity $\mathbf{v}$ is

$$m = m_0 \left(1 - \frac{v^2}{c_0^2} \right)^{\frac{-1}{2}} \tag{43}$$

where m_0 and c_0 respectively denote the particle rest mass and the velocity of light. For particles of charge q_0 the Lorentz force in the laboratory frame is

$$\mathbf{F}_L = \frac{d}{dt}(m\mathbf{v}) = q_0(\mathbf{E} + \mathbf{v} \wedge \mathbf{B}) - \nu_c m\mathbf{v} \tag{44}$$

where a mean collision frequency ν_c has been introduced to take internal friction into account; cf. [6].
Equation (44) is linear in $d\mathbf{v}/dt$ and reads explicitely

$$\frac{d}{dt}(m\mathbf{v}) = m\frac{d\mathbf{v}}{dt} + \mathbf{v}\frac{dm}{dt} = \mathcal{M}\frac{d\mathbf{v}}{dt} = \mathbf{F}_L \tag{45}$$

with

$$\mathcal{M} = m\left(\delta_{ij} + \lambda v_i v_j\right)_{i,j=1,2,3} \quad ; \quad \lambda = \left(c_0^2 - v^2\right)^{-1} \tag{46}$$

by virtue of (43). $\mathcal{M}$ is obviously selfadjoint and strictly positive for $v < c_0$, hence invertible, and yields the relativistic particle acceleration as

$$\dot{\mathbf{v}} = \mathcal{M}^{-1}\mathbf{F}_L \tag{47}$$

Then n particles per unit volume of (mean) velocity $\mathbf{v}$ generate a current density

$$\mathbf{j}_c = \rho \cdot \mathbf{v} \quad ; \quad \rho = nq_0 \tag{48}$$

which has to be included in the generalized Ampère's law (1st Maxwell's integral equation)

$$\int\limits_{\partial A} \mathbf{H} d\mathbf{s} = \int\limits_A \varepsilon \frac{\partial \mathbf{E}}{\partial t} d\mathbf{S} + \int\limits_A \kappa_e \mathbf{E} d\mathbf{S} + \int\limits_A \mathbf{j}_c d\mathbf{S} \tag{49}$$

Charge conservation is ensured by the continuity equation for $(\rho, \mathbf{j}_c)$ or its integral equivalent, the Gauss-Ostrogadski law

$$\int\limits_{\partial C} \mathbf{j}_c d\mathbf{S} = -\frac{d}{dt}\int\limits_C \rho dV \tag{50}$$

valid for arbitrary test volumes C. Of course Faraday's law (Maxwell's 2nd integral equation) holds unalteredly

$$-\int\limits_{\partial A} \mathbf{E} d\mathbf{s} = \int\limits_A \mu \frac{\partial \mathbf{H}}{\partial t} d\mathbf{S} + \int\limits_A \kappa_m \mathbf{H} d\mathbf{S} \tag{51}$$

Perhaps, in the present context the loss currents called forth by the electric and magnetic conductivities κ_e, κ_m in Maxwell's equations (49), (51) attract some attention. They simply allow for simulating dissipative effects of any origin in the plasma. Beyond it, further simplifying assumptions obviously enter the above description, which may be modified or dropped in each case. Thus, the model neglects the direct repulsive Coulomb interaction between

the particles, which amounts to a low density approximation. Also, the fixed mean collision frequency ν_c may be substituted by a state dependent expression.

In the TLM model the physical state, given by the Maxwell field $(\mathbf{E}, \mathbf{H})$, the charge density ρ, and the mean particle velocity $\mathbf{v}$ has to be related to cell states in a suitable interpretation. In a convex hexahedral parcel twines cell (wherein ports on the cell faces interconnect the midpoints of the cell edges, cf. fig.1) the fields are connected to cell states in terms of port voltages and currents

$$U_\mu := \mathbf{E} \cdot \mathbf{p}^\mu \quad , \quad I_\mu := +(-)\mathbf{H} \cdot \mathbf{p}^\nu \tag{52}$$

the sign corresponding with that in

$$\mathbf{f} = +(-)\mathbf{p}^\mu \wedge \mathbf{p}^\nu \tag{53}$$

where $\mathbf{f}$ denotes the cell face vector which points into the cell. On the cell surface U_μ^p, I_μ^p as finite integrals approximate line integrals

$$U_\mu^p \approx \int\limits_{p_\mu} \mathbf{E} d\mathbf{s} \quad ; \quad I_\mu^p \approx +(-) \int\limits_{p_\nu} \mathbf{H} d\mathbf{s} \tag{54}$$

(every port vector in parcel-twines location is naturally identified with an integration path on the pertinent face).

U_μ^n, I_μ^n measure the field strengths *in* the cell according to (52), yet with the nodal images $\mathbf{p}^{\mu,\nu}$, cf. sect.2, (1, 2). The model equations for Ampère's and Faraday's laws are developed in detail in references [12], [14], [15]. A suitable change of representation, cf.[15] sect.4, provides decoupled equations in terms of transformed voltages and currents $(u_\mu^{n,p}, i_\mu^{n,p})_{\mu=1,\ldots,12}$. On the first components $z = (u_\mu, i_\mu)_{\mu=1,\ldots,3}$ the discretized 1st Maxwell equation reduces to

$$\psi_0 z^p\,(t) = \varphi_0 z^n(\, t + \frac{\tau}{2}\,) \; + \varphi_1 z^n(\, t - \frac{\tau}{2}\,) \; + \mathbf{J}_c \tag{55}$$

the convection current $\mathbf{J}_c$ being added here as the following perturbation

$$\mathbf{J}_c = \frac{1}{4}\det(B) B^{-1} \frac{Q}{V} \mathbf{v} = \frac{1}{4} B^{-1} Q \mathbf{v} \tag{56}$$

Q is the total charge in the cell and $\mathbf{v}$ the mean particle velocity. The node vector matrix B with adjoint B_* is defined in reference [15] and (modulo a factor 4) also in reference [14]. In the present normalization the determinant of B equals the cell volume and $A = \det(B) B_*^{-1}$ is the so called area matrix, cf.[15] sect.3.
Still $Q = \rho V$ and $\mathbf{v}$ have to be incorporated into the TLM model as cell state functions. This is achieved by introducing six additional ports in the form of the cell face vectors $\mathbf{f}^\mu$ which measure the convection currents through

the respective cell boundary faces and through pertinent image areas in the node.The link states associated with these ports are

$$\mathbf{J}_\mu := \begin{pmatrix} J_{in} + J_{out} \\ J_{in} - J_{out} \end{pmatrix} \tag{57}$$

to which the following interpretation is construed

$$J_\mu := \mathbf{J}_{\mu,1} = J_{\mu,in} + J_{\mu,out} = \rho \mathbf{v} \cdot \mathbf{f}^\mu \tag{58}$$

Note that voltages are not defined in parallel with these currents. This amounts to neglect a pressure in the here adopted low density i approximation. In transmission line parlance, the characteristic impedance i $\mathfrak{z}$ of the cell face channels is zero, just as then are the voltages $U_n = \mathfrak{z} J_{n,2}$, to which a pressure $p = \rho U$ is assigned. The generalized TLM scheme, which in the setting of sect.3 dispenses with impedances, still works for $\mathfrak{z} = 0$ with link states defined as in (57). The total charge Q in a cell is related to the cell boundary current by charge conservation cf. (47), which yields the updating instructions

$$Q\left(t+\tau\right) = Q(t) + \tau \sum_{\mu=1}^{6} J_\mu^p(t) \tag{59}$$

In the cited canonical representation, [15] sect.4, the nodal states $z_k^n = (u_k^n, i_k^n)$ are interpreted as field strengths

$$\mathbf{E} = B_*^{-1} \left(u_k^n\right)_{k=1,2,3} \quad ; \quad \mathbf{H} = B_*^{-1} \left(i_k^n\right)_{k=7,8,9} \tag{60}$$

These substituted in equation (44) yield the Lorentz force and updated particle velocities in the cells

$$\mathbf{v}(t+\tau) = \mathbf{v}(t) + \tau \mathcal{M}^{-1} \mathbf{F}_L \tag{61}$$

for $\mathcal{M}(\mathbf{v})$, $\mathbf{F}_L(\mathbf{v}, \mathbf{E}, \mathbf{H})$, and $\mathbf{v}$ at time t.

Ultimately, equations (55), (58), (59), (61) are simultaneously solved by deflection, branching out the trivial process $J^n(t) \equiv 0$ and the reflection map $\mathcal{R}$ of the free Maxwell field model as outlined in sect.4. This results in the following updating instructions for the coupled TLM process

$$z_{out}^p(t+\tau) := z_{in}^p(t) + \mathcal{R}[z_{in}^p] + \mathcal{D}(t) \tag{62}$$

$$q := Q(t) + \tau \sum_{\mu=1}^{6} J_{\mu,in}^p(t) \tag{63}$$

$$\mathbf{v}(t+\tau) := \mathbf{v}(t) + \tau \mathcal{M}^{-1} \mathbf{F}_L \tag{64}$$

$$\mathbf{J}_c := \frac{1}{4} B^{-1} q \mathbf{v} \tag{65}$$

$$\mathcal{D}(t+\tau) := \left(\pi_{out} \circ \varphi_0\right)^{-1} \left\{\left(\psi_0 - \varphi_1\right) \mathcal{D}(t) + \mathbf{J}_c\right\} \tag{66}$$

$$J_{\mu,out}^p(t+\tau) := -J_{\mu,in}^p(t) + \det(B)^{-1} q \mathbf{v} \cdot \mathbf{f}^\mu \tag{67}$$

$$Q(t+\tau) := q + \tau \sum_{\mu=1}^{6} J_{\mu,out}^p(t+\tau) \tag{68}$$

with all operations carried out in this order.

Stability requires the assignments must be contractive in the domain of operation (i.e. up to any allowed maximum excitation). This is ensured with bounds for the time step following the guide-lines of sect.6.

A. Appendix

To remain technically in contact with the familiar framework (which uses line impedances) the bridge is thrown in this passage from Maxwell's equations in the transmission line setting [12], [14], [15] to the presently generalized formulation that works with projections instead. In the canonical representation of the link state space, [15] sect.3, with

$$z = \begin{pmatrix} \mathbf{u} \\ \mathbf{i} \end{pmatrix} = \begin{pmatrix} \mathbf{u}_{in} + \mathbf{u}_{out} \\ y(\mathbf{u}_{in} - \mathbf{u}_{out}) \end{pmatrix} \tag{69}$$

($y = 1/\mathfrak{z}$ the characteristic field admittance) the generalized Ampère's law discretized in a parcel-twines cell takes the form of equation (11) with

$$\psi_0 = \begin{pmatrix} 0_3 & 1_3 \\ 0_3 & 0_3 \end{pmatrix} \tag{70}$$

($0_n, 1_n$ denote respectively the $n \times n$ zero and unit matrix blocks) and

$$\varphi_0 = \begin{pmatrix} T_+ & 0_3 \\ 0_3 & 0_3 \end{pmatrix} \quad , \quad \varphi_1 = \begin{pmatrix} T_- & 0_3 \\ 0_3 & 0_3 \end{pmatrix} \tag{71}$$

with real selfadjoint (i.e. symmetric) 3×3 matrix operators

$$T_{+(-)} = \frac{1}{4} \det(B) B^{-1} \left(\frac{\kappa_e}{2} + (-) \frac{\varepsilon}{\tau} \right) B_*^{-1} \tag{72}$$

B is the node vector matrix, defined ibid., which depends only on the cell geometry. κ_e and ε denote respectively the electric conductivity and permittivity tensors. With (69) the projections into the incoming and outgoing states related to Ampère's law (separated) are

$$\pi_{in} = \frac{1}{2} \begin{pmatrix} 1_3 & \mathfrak{z} 1_3 \\ y 1_3 & 1_3 \end{pmatrix} \quad , \quad \pi_{out} = \frac{1}{2} \begin{pmatrix} 1_3 & -\mathfrak{z} 1_3 \\ -y 1_3 & 1_3 \end{pmatrix} \tag{73}$$

Proceeding as outlined in sect.5, i.e. substituting for $z^{n,p}$ in equation (11) with operator coefficients (70), (71) the total scattering response of a Dirac pulse, cf. (26), (27), yields the S-matrix blocks $K_A, \ldots, N_A$ pertinent to

the generalized Ampère's law. Modulo gauge transformations (26) they are uniquely determined as

$$
\begin{aligned}
K_A &= \pi_{out} U \pi_{in} \\
N_A &= \pi_s V \pi_s \\
L_A &= \pi_{out} W \left(Id - N_A^2\right)^{\frac{1}{2}} \pi_s \\
M_A &= \pi_s \left(Id - N_A^2\right)^{\frac{1}{2}} W_* \pi_{in}
\end{aligned}
\tag{74}
$$

with

$$
U = \left(\begin{array}{c|c} yT_+^{-1} - 1_3 & 0_3 \\ \hline 0_3 & -yT_+^{-1} + 1_3 \end{array}\right) \quad , \quad V = -\, yT_+^{-1} - T_+^{-1} T_- \tag{75}
$$

W maps the stub vectors pertinent to Ampère's law back into the link channels and acts in the canonical representation on $z_l^n \oplus z_s$ as a matrix operator

$$
W = \pi_l^n W \pi_s = 2 \left(\begin{array}{c|c} 0 & 1_3 \\ \hline 0 & 0 \end{array}\right) \tag{76}
$$

It is left as an exercise to show that $S_A^{\sim}$ with these data is unitary iff $\kappa_e = 0$.

For Faraday's law the derivation of operators $K_F \ldots N_F$ runs completely parallel.

2. Conclusions

Despite the rich potentiality they offer, the gauge properties of the TLM scheme remain still largely unexploited, today, in numerical model design. A general method that allows for incorporating a linear or non-linear interaction into a given linear model using these properties has been developed in this paper, on the algorithmic level and within a prototype application.

From a fundamental point of view, future work should yield still deeper insight into the precise nature and the range of the observed gauge similarity. It is clear from the preceeding that the latter is not to be (mis)understood in the restricted sense of Lagrangian field theory: Until now, a *Lagrangian* is not known in the TLM context (though it may be challenging to look for such an object). Instead, the structural relationship traced out points to some more general common aspects: Much alike gauge field models, the TLM algorithm works with unobservable quantities that intermediate interactions and which together with their internal symmetries can be similarly described in fibrations. There is a considerable differential geometric overlap with gauge field theory that attracts our attention and further study in this direction may significantly promote the TLM method.

Ultimately, not a few technical spade-work of course remains to be done in any particular application that is conceivable. The propagator approach marks only a canonical path equipped with reliable instruments.

References

[1] Christopoulos, C. *The Transmission-Line Modeling Method TLM*, IEEE Press, New York 1995

[2] De Cogan, D. *Transmission Line Matrix (TLM) Techniques for Diffusion Applications*, Gordon and Breach, 1998

[3] Lax, P.D. and Phillips, R.S. *Scattering Theory*, Academic Press, New York 1967

[4] Mandl, F. and Shaw G. *Quantum Field Theory*, John Wiley & Sons, Chichester 1984

[5] Mayer M.E. and Drechsler, W. *Fiber Bundle Techniques in Gauge Theories, Lecture Notes in Physics*, 67, Springer-Verlag, Heidelberg 1977

[6] Cap, F. *Lehrbuch der Plasmaphysik und Magnetohydrodynamik*, Springer-Verlag, Wien 1994

[7] Johns, P.B. and Beurle, R.L. Numerical solution of 2-dimensional scattering problems using transmission line matrix, Proc.IEEE, 118, pp. 1203-1208, 1971

[8] Hoefer, W. The Transmission Line Matrix (TLM) Method, Numerical Techniques for Microwave and Millimeter-Wave Passive Structures, ed. Itoh, T., John Wiley & Sons, New York 1989

[9] De Cogan, D. and Enders, P. Discrete Models of Heat Flow in Layered Materials Using Simple and Correlated Random Walks, Int. J. Num. Modelling, vol. 9, pp. 445-457, 1996

[10] Witwit, A.R.M. Wilkinson, A.J. and Pulko, S.H., A Method for Algebraic Analysis of the TLM Algorithm, Int. J. Num. Modelling, vol. 8, pp. 61-71, 1995

[11] Hein, S. Consistent finite difference modelling of Maxwell's equations with lossy symmetrical condensed TLM node, Int. J. Num. Modelling, vol 6., pp. 207-220, 1993

[12] Hein, S. Finite difference time domain approximation of Maxwell's equations with non-orthogonal condensed TLM mesh, Int. J. Num. Modelling, vol. 7., pp. 179-188, 1994

[13] Hein., S. A TLM node for superconducting boundary illustrating the propagator approach, Spinner Report E017, München 1992

[14] Hein, S. TLM Numerical Solution of Bloch's Equations for Magnetized Gyrotropic Media, Appl. Math. Modelling, vol. 21, pp. 221-229, 1997

[15] Hein, S. Synthesis of TLM algorithms in the propagator integral framework, invited paper, Proc. 2nd Int. Workshop on Transmission Line Matrix (TLM) Modelling, TU München, pp. 1-11, 1997

Steffen Hein; DE-83043 Bad Aibling, Germany
E-mail address: steffen.hein@bnro.de